Upcycling Waste Tempura Flake-derived Starch Powder as an Environment-Friendly Polymer Matrix Filler for Thermoplastic Starch Compounds

Seunghyun Yoo,[a] Seungho Lee,[a] Sung-Won Kang,[b,*] and Kwang-Ho Ahn [b,*]

Waste tempura flakes collected from local restaurants were upcycled to be utilized as a polymer filler material. The oil fraction in collected waste tempura flakes were extracted two times *via* centrifugal solid-liquid separation and organic solvent extraction. Then, oil-extracted residual starch was freeze-milled to produce fine powders. Waste tempura flake-derived starch powder was substituted with 1%, 3%, and 5% (wt%) of virgin starch powder to produce thermoplastic starch. Composition, X-ray diffraction, and Fourier transform infrared analyses showed that the mixture was successfully thermally plasticized. Substitution of waste tempura flake-derived starch decreased tensile strength while increasing elongation at break of some samples. Produced thermoplastic starch samples again were compounded with polylactic acid (PLA) and poly-butylene adipate-co-terephthalate (PBAT) following a mixing ratio of 3:5:2. The analyses indicated that thermoplastic starch, PLA, and PBAT were successfully compounded. The compound containing 1 wt% substituted thermoplastic starch showed the minimal mechanical strength decrease. This study revealed the possibility of upcycling waste fried food into a valuable bioplastic material. Waste tempura flakes can be utilized as both bio-jet fuel and bioplastic filler material.

DOI: 10.15376/biores.19.1.1394-1409

Keywords: Waste tempura flake; Waste upcycling; Thermoplastic starch; Filler; Bioplastic; Compounding

*Contact information: a: R&D Team, The Day1Lab, #1017 Mario Tower, 28 Digital-ro 30-gil, Guro-gu, Seoul, 08389, Republic of Korea; b: Department of Environmental Research, Korea Institute of Civil Engineering and Building Technology, 283, Goyang-daero, Ilsanseo-gu, Goyang-si, Gyeonggi-do, 10223, Republic of Korea; *Corresponding authors: kangsw93@kict.re.kr, khahn@kict.re.kr*

INTRODUCTION

During the COVID-19 pandemic, the food delivery service became popular to minimize exposure among unknown people and prohibit dissemination of the virus. However, the increased popularity of food delivery service had a downside regarding plastic waste generation (Adyel 2020; Shams *et al*. 2021). According to the Korea Environment Corporation, the plastic waste generation per Seoul citizen doubled from 110 g in 2016 to 236 g in 2020. Furthermore, among different industries, the plastic industry is ranked 3rd place regarding carbon emissions. To solve the issue, biodegradable plastics, such as PBAT (poly(butylene adipate-co-terephthalate), and PBS (polybutylene succinate) resins, were actively introduced to the conventional plastic market (Dilkes-Hoffman *et al*. 2019). PLA only degrades under industrial composting conditions including temperatures of 50 to 70 °C and high moisture content (Anderson and Shenkar 2021). Home, soil, and marine composting are not accepted for the degradation of PLA. These materials were advertised as decomposing under industrial or home compostable conditions. However,

Purkiss *et al*. (2022) tracked home and industrial compostable products sold in the United Kingdom and it turned out that 55% of products did not decompose enough to fulfill the certification criteria. To overcome the weakness of conventional biodegradable plastics, utilization of biomass has received much attention in industries and academia (Coppola *et al*. 2021; Kawaguchi *et al*. 2022).

Biomass refers to a living organism-derived organic product that consists of polysaccharide backbone, lipids, proteins, extractives, and inorganics (Bonechi *et al*. 2017). Biomass has versatile applications such as construction materials, paper feedstock, bioenergy feedstock, composite materials, and platform chemical feedstock (Brinchi *et al*. 2013; Jiang *et al*. 2021; Okolie *et al*. 2021). Among several different biomasses, starch attracted attention from the polymer industry because of its thermal processability and cheap price (Mohammadi Nafchi *et al*. 2013; Mendes *et al*. 2016). Starch itself has been used as a filler for petroleum-derived plastic polymers (Santos *et al*. 2023). However, the only benefit of using starch as a simple filler is manufacturing cost reduction. As more starch powder is added to the main polymer matrix, mechanical properties are deteriorated (Santos *et al*. 2023). Other disadvantage of compounding starch and biomasses with petrochemical plastic is increased generation of microplastics and nanoplastics, Accordingly, the compounding of biomass and petrochemical plastics is not recommended for environmental purposes (Rahardiyan *et al*. 2023).To overcome the drawback of simple starch filler, a thermally flowing form of starch was developed. Combined with plasticizer, heat, and pressure, raw starch powder turns into a yellowish or brownish flowing viscous matter called thermoplastic starch (TPS) (Mohammadi Nafchi *et al*. 2013). The color of TPS may range from yellow to brown depending on extrusion conditions including temperature, rpm of screw, and feeding speed (Iriani *et al*. 2012; Hazer and Aytac 2023). When TPS is extruded with other polymers to make composites, it is more compatible with other polymers compared to starch filler (Cuevas-Carballo *et al*. 2019; Garalde *et al*. 2019). Furthermore, in terms of mechanical properties, TPS-containing composites show better performances compared to those of starch filler containing composites.

Recently, several studies have been conducted regarding upcycling waste starch materials. Starch-based polysaccharides can be hydrolyzed into monosaccharides, such as glucose, which can then be fermented using microorganisms to produce alcohols through fermentation of sugars derived from enzymatic hydrolysis treatment of food wastes (Jesse *et al*. 2002; Kheyrandish *et al*. 2015; Onyeaka *et al*. 2022). Residual starch from flour wet milling, supplemented with crushed wheat grains, was hydrolyzed for ethanol production by *Zymomonas mobilis* ZM4 and an industrial ethanol-producing strain of *Saccharomyces cerevisiae* (Jesse *et al*. 2002). Fermentation of a rice starch waste doped with orange peel was investigated for the enhanced biobutanol production using an amylolytic *Clostridium* in a defined mineral salts medium (Su *et al*. 2022). Starch saccharification by α-amylase (amyA) allows strain T34-N4 to grow and directly produce polyhydroxybutyrate (PHB) from cheap waste starch materials, such as cassava pulp and oil palm trunk starch (Bomrungnok *et al*. 2020). The production of pullulan from hydrolyzed potato starch waste by *Aureobasidium pullulans* P56 was investigated to optimize process variables (incubation time, initial substrate concentration, and initial pH) (Barnett *et al*. 1999; Göksungur *et al*. 2011).

Oil fried food specifically containing carbohydrates is one of the most consumed foods around the world. The amount of fried food waste from the food industry is estimated as several hundreds of millions of tons from worldwide. Because most of the waste from fried food does not easily decompose, a post treatment is required to avoid oil-derived

environmental pollutions. Considering the high oil content of waste fried food, a large amount of residual oil can be extracted from the waste fried food to be utilized as a biodiesel feedstock *via* the chemical process (Fonseca *et al.* 2019). The biofuel enforcement by the United States government results in carbon dioxide emission reduction as 20 million metric tons per year, which is equivalent to the carbon tax saving of $20 per ton. The mandated substitution of biofuels significantly reduces the usage of petroleum-derived products (Johansson *et al.* 2020). Considering the lower oil extraction process cost from the industrial food waste and easy-decaying nature of oil fraction when added to plastic, utilizations of extracted oil fraction as jet fuel substitute and waste solid starch fraction as bioplastic filler are economically plausible (Sakuragi *et al*. 2016).

Because most of the solid fraction of waste fried food remains after extraction of oil, it can be used for waste upcycling (Johansson *et al*. 2020). Existing studies regarding upcycling of waste from fried food has focused on utilization of oil/fat fraction, thermochemical conversion, and biochemical conversion. No research has been conducted regarding direct application of solid waste fraction, which consists of polysaccharide or denatured polysaccharide. This study will thoroughly investigate upcycling of residual starch from waste tempura flake.

EXPERIMENTAL

Materials Preparation – Oil Extraction from Waste Tempura Flake

Waste tempura flake was collected from local restaurants (Cheong-ju, South Korea). Collected waste tempura flake was pretreated to perform the primary oil extraction from the waste. About 100 g of waste tempura flake was dispersed in 1,000 mL of 90 °C water by soaking it for 10 min and then stirred at 200 rpm to make tempura flake slurry. The tempura flake slurry was centrifuged for 15 min at 4,500 rpm to separate oil fraction, water, and residual starch fraction. The residual starch fraction was again soaked in 50 °C water and centrifuged 5-more times to maximize the oil extraction from the residual starch fraction. After 5 times of extraction at 4,500 rpm, the residual starch was vacuum dried and milled into a powder for use in further experiments.

Secondary oil extraction was performed using Soxhlet and an organic solvent (Ramluckan *et al*. 2014). About 42 g of primary oil-extracted dried residual starch was stored in a cellulose thimble and 420 mL of 1:2 ethanol-ether mixed solvent (by volume) was poured into the thimble for Soxhlet extraction. The Soxhlet was heated for 6 h at 80 °C. After the secondary extraction, the residual starch fraction was oven dried and weighed to calculate the extracted oil mass fraction. Although oil can function as lubricant, primary and secondary oil extraction are required because the oil fraction in waste tempura flake decays during the practical application of products.

Materials Preparation – Freeze Milling

A 6875D FREEZER-MILL (SPEX SamplePrep, Yongin, South Korea) was utilized to reduce the particle size of the primary and secondary oil-extracted residual starch. About 60 g of residual starch was loaded in the chamber of the mill and liquid nitrogen was filled in the chamber. After closing the chamber, power is applied to the coil surrounding the chamber to induce a magnetic field, which activates a rod-shaped steel impactor to mill the sample into fine powder.

Thermoplastic Starch and Compound Extrusion

A BA-19 twin extruder (BauTek, Pocheon, South Korea) was utilized to produce TPS and derived compounds (Cuevas-Carballo *et al*. 2019; Garalde *et al*. 2019; Katanyoota *et al*. 2023). Corn starch (Sigma Aldrich, Seoul, South Korea) and glycerine (Duksan, Seoul, South Korea) were used for thermoplastic starch extrusion. Polylactic acid (PLA, LX175, Total Corbion, Seoul, South Korea) and polybutylene adipate terephthalate (PBAT, ANKOR, South Korea) were purchased for compounding of waste tempura flake-derived starch added bioplastic compound.

Elemental Analysis

Carbon, hydrogen, and nitrogen contents of the bioplastic samples were analyzed using a Vision-EA elemental analyzer (Isoprime, UK). Oxygen content was calculated by difference.

Thermogravimetric Analysis

Proximate analysis was performed to determine volatile matter and fixed carbon fractions using a Discovery TGA 5500 thermogravimetric analyzer (TA Instruments, Seoul, South Korea). The specific measurement method mentioned in ASTM D7582-15 (2023).

Melt Flow Index

Melt flow index (MFI) is basically defined as the weight of the polymer (g) extruded in 10 min through a capillary of specific diameter and length by pressure applied through dead weight under prescribed temperature conditions. ASTM D1238 (2013) describes the test conditions for general purpose polymers. The test conditions include the onset temperatures as 190 °C and 2.16 kg of weight apply.

Mechanical Strength Measurement

The tensile properties were measured in accordance with ASTM D638-96 (2022) type II requirements. Tensile bars made by the hot press mold process described earlier were conditioned at 25 ± 1 ℃ and 53% RH for at least 48 h before performing tensile tests. Tensile tests were conducted using a universal test instrument equipped with 500 kg load cell and operated at a crosshead speed of 5 mm/min. The tensile modulus was calculated from the slope of the initial and linear region of stress–strain curves. A minimum of five specimens were tested and the average values and standard deviations were reported.

X-ray Diffraction Analysis

X-ray diffraction patterns of TPS and their compounds were collected using a SmartLab X-ray diffractometer (Rigaku, Seoul, South Korea). Operating voltage was 40 kV and operating current was 44 mA. A Cu Kα X-ray tube was used to generate X-rays at a wavelength of 0.1541 nm. A Graphite monochromator and Kβ filter were used for the collection of diffracted beams. Thermoplastic starch and compound pellet samples were placed on a glass sample holder. Then, the sample holder was placed inside the X-ray chamber. Measurement of 2θ angle range was set from 10° to 40°. Each step was 0.05 degrees and the X-ray detector remained constant for 4.5 s at each step to collect the diffracted X-rays.

Fourier Transform Infrared (FT-IR) Analysis

The FT-IR measurements were performed in the mid-infrared region (4000 to 650 cm^{-1}) using a Nicolet 6700 (Thermo Scientific Co., Seoul, South Korea) FT-IR spectrophotometer, configured with an attenuated total reflectance (ATR) mode. Thermoplastic starch and compound samples were placed on a diamond crystal sampling plate and clamped with a pointed tip. A background scan was obtained before every sample scan with an empty sample plate. A total of 128 accumulative scans from each sample were collected at 4 cm^{-1} intervals, and average spectra intensity was used for further analysis.

RESULTS AND DISCUSSION

Oil Extraction from Waste Tempura Flake and Particle Size Reduction for Bioplastic Application

The waste tempura flake contains 44.7 wt% of residual starch, 48 wt% of centrifuge-extractable oil, and 7.3 wt% of organic solvent-extractable oil fractions. The waste tempura flake was first soaked in tap water for the primary oil-extraction *via* centrifuge. After the centrifuge step, 48% of oil was extracted and 52% of the feedstock was left as the primary residual solid, which consists of cooked starch and organic solvent-extractable oil. The primary oil-extracted residue was further treated with 1:2 ethanol-ether mixed solvent (by volume) to further extract starch bound oil fraction. Organic solvent extraction was able to extract 7.3% of extra oil fraction from the primary residual starch. After 2-step of oil extraction, less than 0.75% of oil remained in the starch. The organic solvent-extracted residual starch is referred to as the secondary oil-extracted residual starch. After the second oil extraction, the residual starch powder became less oily, and the color turned into bright brownish.

The primary and secondary oil-extracted residual starch samples went through freeze drying and milling process to reduce the particle size for the further extrusion process. Figure 1 shows freeze-milled primary and secondary oil-extracted residual starch samples. Reduced particle size of residual starch promotes the plasticizing activity during the twin extrusion process.

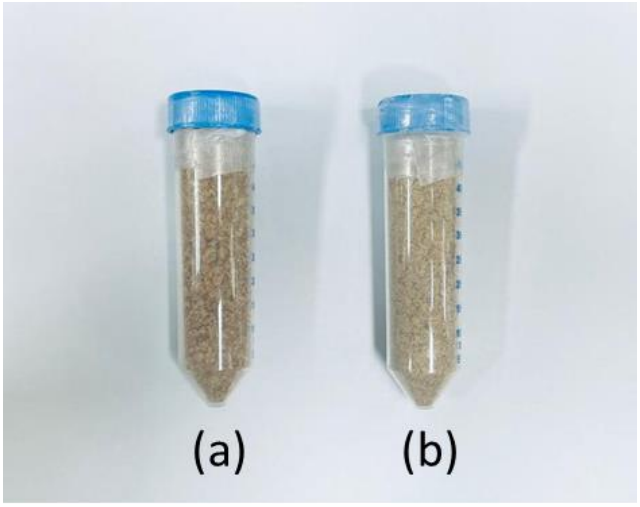

Fig. 1. Freeze-milled primary (a) and secondary (b) oil-extracted residual starch samples

Thermoplastic Starch Extrusion and Compounding with Other Bioplastics

Freeze-milled oil-extracted residual starch samples were mixed with raw starch and glycerine for the TPS extrusion. The mixing ratio of raw materials is given in Table 1. About 1%, 3%, and 5% (wt%) solutions of the primary and secondary oil-extracted residual starch powders were mixed with virgin starch fraction for TPS extrusion.

Table 1. Thermoplastic Starch Mixing Ratio

Wt%	TPS Control	TPS E1-1	TPS E1-2	TPS E1-3	TPS E2-1	TPS E2-2	TPS E2-3
Starch	65	64	62	60	64	62	60
Glycerine	35	35	35	35	35	35	35
Primary Oil-Extracted Residual Starch	-	1	3	5	-	-	-
Secondary Oil-Extracted Residual Starch	-	-	-	-	1	3	5

Thermoplastic starch samples added with primary and secondary oil-extracted residual starch were again compounded with PLA and PBAT. Their compound ratio was TPS:PLA:PBAT = 3:5:2 by weight. Figure 2 shows the sample images of all TPS samples and their bioplastic compounds. As more oil-extracted residual starch powder is added to TPS, the color of both TPS and their compounds (CPD) turned dark brownish.

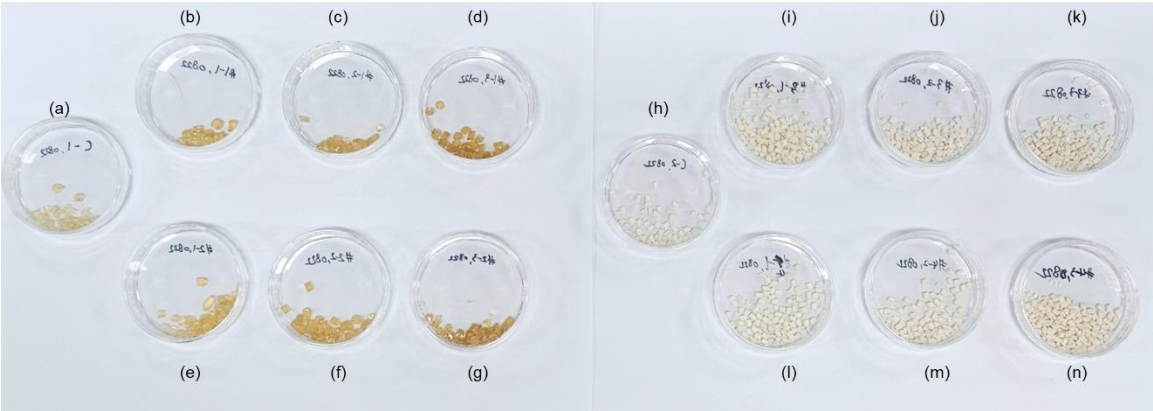

Fig. 2. Photo of thermoplastic starch samples ((a) TPS control, (b) TPS E1-1, (c) TPS E1-2 (d) TPS E1-3, (e) TPS E2-1, (f) TPS E2-2, (g) TPS E2-3) and bioplastic compound samples ((h) CPD Control, (i) CPD E1-1, (j) CPD E1-2, (k) CPD E1-3, (l) CPD E2-1, (m) CPD E2-2, (n) CPD E2-3)

Elemental and Proximate Composition Analysis of TPS and Their Compounds

Elemental and proximate analyses were performed to scrutinize the chemical composition and bulk property of TPS and their compounds (Yoo *et al*. 2018). Elemental and proximate composition data are given in Table 2. Comparison among TPS samples show that carbon, hydrogen, and oxygen contents remained almost the same regardless of oil-extracted residual starch addition. However, the nitrogen content increased as more oil-extracted residual starch were added to the TPS matrix. The increased nitrogen content may originate from food ingredients used for pan frying (Pokorny 1998). The increment of nitrogen content was higher from the secondary oil-extracted residual starch samples. In

contrast, the elemental compositions of compound samples showed similar values regardless of oil-extracted residual starch addition.

Proximate analysis, which reveals the bulk physicochemical property of organic materials, also showed differences among thermoplastic starch samples (Yoo *et al*. 2018). Addition of both primary and secondary oil-extracted residual starch increases the fixed carbon content while decreasing the volatile matter content.

Table 2. Elemental and Proximate Composition of Thermoplastic Starch and Thermoplastic Starch-Derived Compounds

	Elemental Composition (%)				Proximate Composition (%)	
	C	H	O	N	Volatile Matter	Fixed Carbon
TPS Control	41.71	7.85	50.42	0.01	94.59	5.41
TPS E1-1	41.93	7.53	50.53	0.01	94.64	5.36
TPS E1-2	41.72	7.46	50.79	0.03	94.04	5.96
TPS E1-3	41.62	7.44	50.88	0.05	93.60	6.40
TPS E2-1	41.49	7.46	51.03	0.02	94.39	5.61
TPS E2-2	41.70	7.50	50.78	0.02	93.54	6.46
TPS E2-3	41.45	7.57	50.91	0.07	94.21	5.79
CPD Control	52.83	6.53	40.63	0.01	97.90	2.10
CPD E1-1	52.24	6.49	41.26	0.01	94.17	5.83
CPD E1-2	52.16	6.40	41.43	0.01	97.99	2.01
CPD E1-3	52.36	6.46	41.16	0.01	97.60	2.40
CPD E2-1	51.10	6.29	42.59	0.01	97.25	2.75
CPD E2-2	51.89	6.42	41.67	0.01	96.61	3.39
CPD E2-3	51.39	6.34	42.26	0.01	96.76	3.24

Mechanical and Thermal Properties of TPS and their Compounds

Mechanical properties including tensile strength and elongation at break were measured for both TPS and their derivative compounds. The data sets are given in Figs. 3 and 4. Two different trends were observed. For TPS substituted with the primary and secondary oil-extracted residual starches, all samples experienced a decrease in tensile strength from 4.2 to the range 1.4 to about 2.1 MPa. However, the substitution of 1% and 3% of the primary oil-extracted residual starch and 1% of the secondary oil-extracted residual starch resulted in an increase in elongation at break from 48.5% to 72.8% to 83.2%. A small fraction substitution of oil-extracted residual starch can enhance the elongation property of thermoplastic starch.

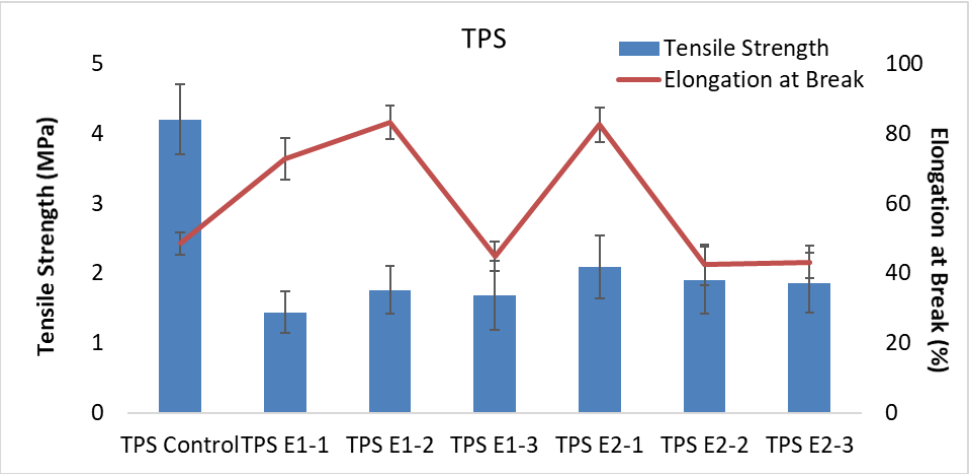

Fig. 3. Tensile strength and elongation of thermoplastic starch samples

A different trend was observed from compound samples. Both tensile strength and elongation at break decreased as more oil-extracted residual starch was substituted in the compound. The sample CPD E2-3, containing 20% TPS E2-3, recorded the lowest tensile strength and elongation at break as 28.1 MPa and 10.21%, respectively. The highest mechanical strength properties were measured from CPD E2-1 as 2.09 MPa and 69.0%. Compared to those of control sample, the tensile strength drop was 1.8% and the elongation at break drop was 29%. The CPD E2-1 mixing composition gives a possibility for using waste tempura-derived starch as a cheap thermoplastic starch filler. It is assumed that oil-extracted residual starch's thermoplastic ability is lower than that of virgin starch. Melt flow index, FT-IR, and XRD results will allow further examination of this phenomenon.

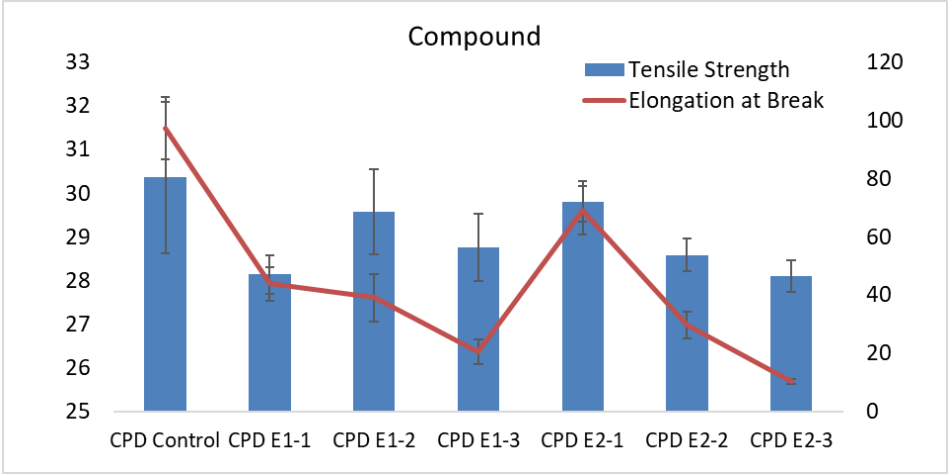

Fig. 4. Tensile strength and elongation of thermoplastic starch-derived compound samples

Melt flow index (MFI) gives indirect physical and chemical structure of polymer matrix *via* representing its flowability under applied temperature and pressure conditions. The MFI value of TPS control was measured as 6.16 g/10 min. The TPS E1-1 sample, containing 1% primary oil-extracted residual starch, showed an MFI value as 7.13 g/10 min, which is higher than that of the control sample.

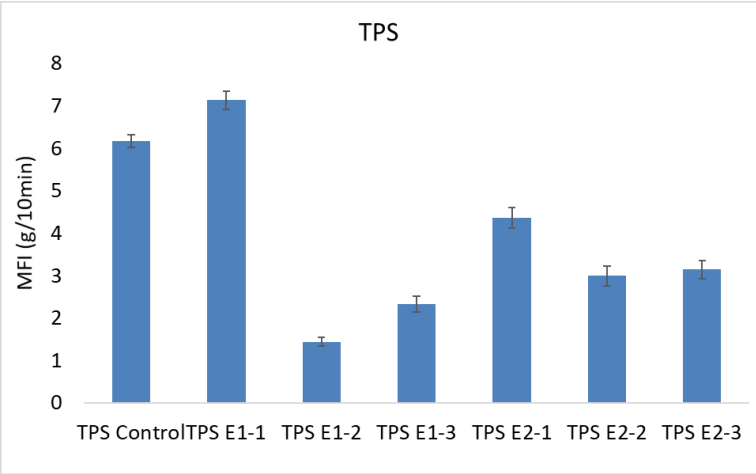

Fig. 5. Melt flow index values of thermoplastic starch samples

For compounds, MFI values were measured in between 4.6 and 4.78 g/10 min. Substitution of different types of TPS slightly increased the thermal flowability of TPS, PLA, and PBAT compound. Inside the matrix, oil-extracted residual starch works as a lubricant (Lee *et al*. 2006).

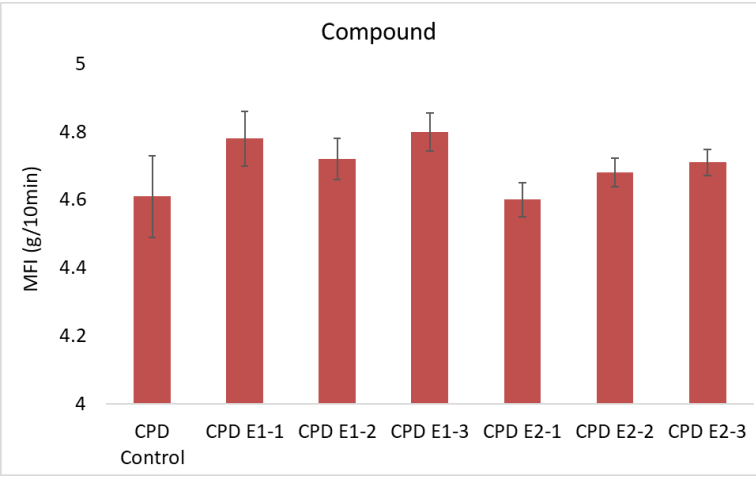

Fig. 6. Melt flow index values of thermoplastic starch-derived compound samples

Physical Structure Analysis of Thermoplastic Starches and Compounds by X-Ray Diffraction

X-ray diffraction patterns of TPS and compounds are given in Figs. 7 and 8. These XRD patterns are evidence of the degree of TPS thermoplasticity and TPS compatibility with other bioplastic components. The XRD patterns of thermoplastic starches (Fig. 7) showed a wide amorphous pattern from 8.3° to 30.7° and semi-crystalline patterns at 13.7°, 18.1°, 19.65°, 20.85°, 25.6°, and 30.7°. The 2θ angles at 13.7° and 20.85° were originated from the amylose-glycerol complex crystal structure, which is also known as Vh-type crystal (Mendes *et al*. 2016; Chen *et al*. 2019). The presence of Vh-type crystal shows that the starch-based matrices containing oil-extracted residual starch were well converted into thermoplastic conformation. The 2θ angles at 18.1°, 19.65°, 25.6°, and 30.7° are designated to B-type crystals, which are typical patterns of stored TPS (Pérez and Bertoft 2010;

Mendes *et al*. 2016; Martens *et al*. 2018). Characteristic 2θ angles derived from A-type crystal of native corn starch found at 15°, 17°, and 23° were missing from the XRD pattern. Disappearance of A-type crystal-related XRD patterns demonstrated that all starch samples were successfully converted into TPS form (Pérez and Bertoft 2010; Dome *et al*. 2020). When starch was fried and oil-extracted, measurements recorded the appearance of similar XRD 2θ angle positions as those of TPS control sample. A similar XRD pattern observation before and after starch frying was reported by Chen *et al*. (2018). Due to the similarities in crystal structure of TPS control and oil-extracted starch containing samples, particle size and the amount of residual oil fraction could affect mechanical properties (Lv *et al*. 2019).

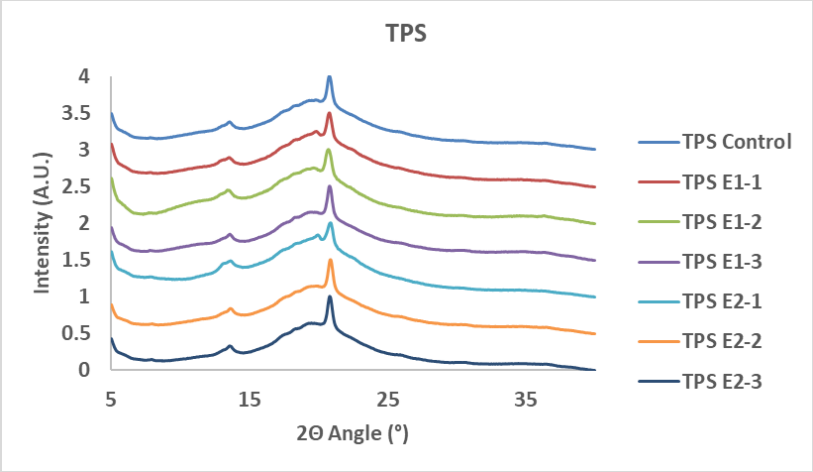

Fig. 7. Co-plotted X-ray diffraction patterns of thermoplastic starch samples

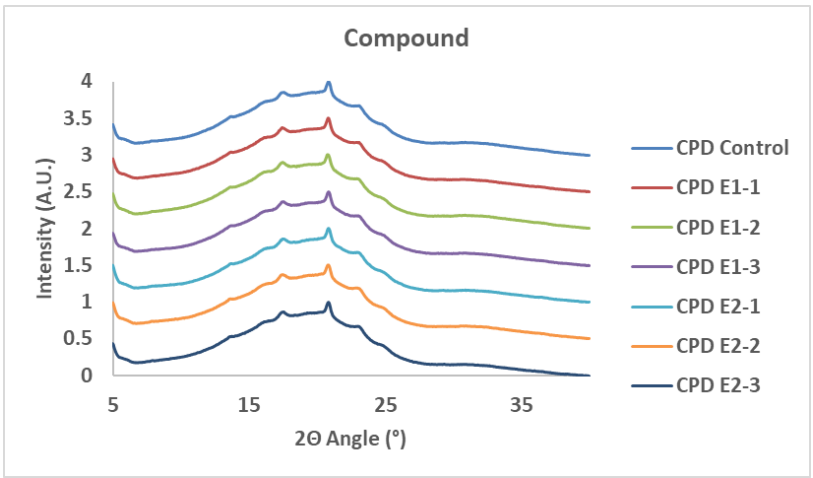

Fig. 8. Co-plotted XRD patterns of thermoplastic starch-derived compound samples

X-ray diffraction patterns of compounds also showed a broad amorphous pattern from 8.75° to 27.85° in 2θ angles range. Semi-crystalline patterns are found at 13.65°, 16.3°, 17.85°, 20.95°, 23.2°, 25.2°, and 30.75°. These XRD patterns are complex convolution of TPS, PBAT, and PLA. The LX175(PLA) exhibited a broad semi-crystalline XRD pattern from 10° to 27° of 2θ angles window (Cardoso *et al*. 2019; Mortalò *et al*. 2023). The XRD patterns of PBAT showed peaks at 2θ values at 16.3°, 17.7°, 20.5°, 23.4°, and 25.3°. Compared to other studies that analyzed the structure of TPS-PLA-PBAT compound, the XRD patterns from this study showed a similar trend (Cardoso *et al*. 2019;

Garalde *et al*. 2019). Overall XRD patterns of TPS-PLA-PBAT compounds indicated that the components were well blended with superior compatibility.

Chemical Structure Analysis of Thermoplastic Starches and Compounds by FT-IR

The FT-IR spectra of TPS and compounds are given in Figs. 9 and 10. Absorbance spectra of TPS reveals functional groups in starch and glycerine (Mecozzi *et al*. 2012). The broad peak at 3,200 to 3,300 cm^{-1} represents –OH group vibration (mostly derived from –OH group in raw starch), the doublets at 2,935 cm^{-1} represent asymmetrical stretching of CH_3, the broad peak at 1,370 cm^{-1} represents symmetrical bending of CH_3, multiple peaks at 1,173, 1020, and 964 cm^{-1} represent the C-O and C-O-C stretchings of polysaccharide, and the peak at 1,420 cm^{-1} is related to the vibration mode of glycerine. The FT-IR spectra of TPS given at Fig. 9 reveals stereotypical thermoplastic starch.

When oil is extracted from fried starch, a significant IR intensity decrease in 1,743 cm^{-1} is found (Chen *et al*. 2018). The peak is related to molecular bonding between oil and starch that the increased elongation at break values of TPS E1-1 and TPS E1-2 samples are originated from the lubricating effect of residual oil fraction.

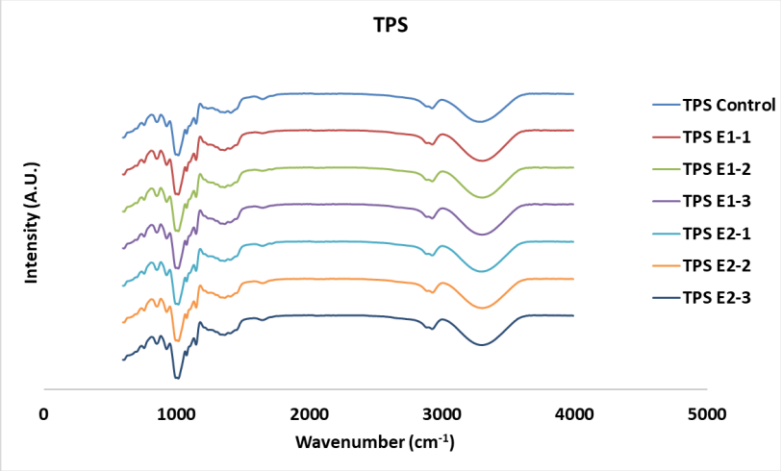

Fig. 9. Co-plotted FT-IR spectra of thermoplastic starch samples

When it comes to the FT-IR spectra of TPS-PLA-PBAT compound, some new peaks were observed. The broad band at 3,200 to 3,300 cm^{-1} related to the –OH group vibration disappeared and an overlapped peak at 1,735 cm^{-1} appeared. The sharp peak at 1,735 cm^{-1} is associated with C-O stretching, which originated from ester bonding in PLA and PBAT (Cuevas-Carballo *et al*. 2019). The small peak at 729 cm^{-1} is associated with C-H bonding vibration attached to benzene ring originated from PBAT (da Silva *et al*. 2019). The peak at 868 cm^{-1} represents vibration of O-CH-CH_3 ester group in PLA (Cuevas-Carballo *et al*. 2019). The peak at 1,030 cm^{-1} originated from surface hydrogen bonding to phenyl ring of PBAT (da Silva *et al*. 2019). Peaks at 1,126 and 1,184 cm^{-1} are vibration modes of C-O and C-O-C bonds from PBAT and PLA each (Cuevas-Carballo *et al*. 2019; da Silva *et al*. 2019). The peak at 1270 cm^{-1} is associated with symmetric stretching of C-O from PBAT (da Silva *et al*. 2019). The peak at 1385 cm^{-1} is a convolution peak of thermoplastic starch and PLA originated from symmetric bending of C-H. Lastly, the peak at 1,454 cm^{-1} originated from antisymmetric mode of CH_3 (Mecozzi *et al*. 2012). The FT-IR spectra of compounds support that three components were well-blended to form a single compound.

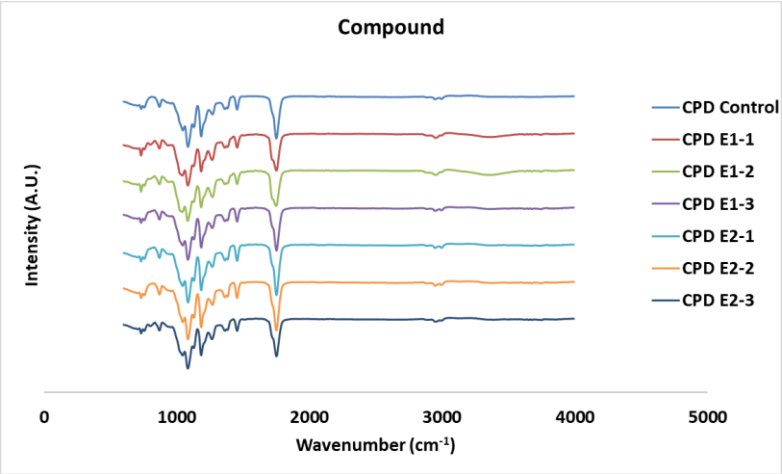

Fig. 10. Co-plotted FT-IR spectra of thermoplastic starch-derived compounds

CONCLUSIONS

1. The composition of market collected waste tempura flake-derived starch consists of 44.7 wt% of residual starch fraction, 48 wt% of centrifuge-extractable oil fraction, and 7.3 wt% of organic solvent-extractable oil fraction.
2. Waste tempura flake-derived oil-extracted residual starch was upcycled as a filler material for thermoplastic starch (1%, 3%, and 5% substitution levels). Thermoplastic starch was successfully extruded and evaluated by composition, X-ray diffraction (XRD), and Fourier-transform infrared (FT-IR) analyses.
3. When thermoplastic starches are substituted with oil-extracted residual starch, tensile strength decreases while elongation at break increases up to 3 wt% substitution compared to those of control sample. Melt flow index increase was found from 1 wt% primary oil-extracted residual starch substituted sample. The rest of samples experienced a decrease in melt flow indices.
4. Thermoplastic starch-poly(lactic acid)-poly(butylene adipate-co-terephthalate) (TPS-PLA-PBAT) compounds were successfully extruded by using oil-extracted residual starch substituted thermoplastic starches. The quality of compounds was scrutinized *via* composition, XRD, and FT-IR analyses.
5. Regarding TPS-PLA-PBAT compounds, tensile strength, and elongation at breaks of all residual starch substituted samples decreased compared to those of control sample. The CPD E2-1 sample showed minimal mechanical strength decrease of 1.8% in tensile strength and elongation at break decrease of 29%. The melt flow index of all samples increased compared to that of control sample. Oil-extracted residual starch acts as lubricant in TPS-PLA-PBAT compound.
6. Considering mechanical and thermal properties, CPD E2-1 composition shows the highest possibility for using waste tempura flake-derived starch as a sustainable bioplastic filler.

ACKNOWLEDGMENTS

This research was funded by the Korea Institute of Civil Engineering and Building Technology (Grant number 20230316-001).

REFERENCES CITED

ASTM D638-96 (2022). "Standard test method for tensile properties of plastics," ASTM International, West Conshohocken, PA, USA.

ASTM D1238 (2013). "Standard test method for melt flow rates of thermoplastics by extrusion plastometer," ASTM International, West Conshohocken, PA, USA.

ASTM D7582-15 (2023). "Standard test methods for proximate analysis of coal and coke by macro thermogravimetric analysis," ASTM International, West Conshohocken, PA, USA.

Adyel, T. M. (2020). "Accumulation of plastic waste during COVID-19," *Science* 369(6509), 1314-1315. DOI: 10.1126/science.abd9925

Anderson, G., and Shenkar, N., (2021). "Potential effects of biodegradable single-use items in the sea: Polylactic acid (PLA) and solitary ascidians," *Environmental Pollution* 268, article ID 115364. DOI: 10.1016/j.envpol.2020.115364

Barnett, C., Smith, A., Scanlon, B., and Israilides, C. J. (1999). "Pullulan production by *Aureobasidium pullulans* growing on hydrolysed potato starch waste," *Carbohydrate Polymers* 38(3), 203-209. DOI: 10.1016/S0144-8617(98)00092-7

Bomrungnok, W., Arai, T., Yoshihashi, T., Sudesh, K., Hatta, T., and Kosugi, A. (2020). "Direct production of polyhydroxybutyrate from waste starch by newly-isolated *Bacillus aryabhattai* T34-N4," *Environmental Technology* 41(25), 3318-3328.

Bonechi, C., Consumi, M., Donati, A., Leone, G., Magnani, A., Tamasi, G., and Rossi, C. (2017). "Biomass: An overview," in: *Bioenergy Systems for the Future*, F. Dalena, A. Basile, and C. Rossi (Eds.), Woodhead Publishing, Sawston, Cambridge, UK, pp. 3-42. DOI: 10.1016/B978-0-08-101031-0.00001-6

Brinchi, L., Cotana, F., Fortunati, E., and Kenny, J. M. (2013). "Production of nanocrystalline cellulose from lignocellulosic biomass: Technology and applications," *Carbohydrate Polymers* 94(1), 154-169. DOI: 10.1016/j.carbpol.2013.01.033

Cardoso, E. C., Parra, D. F., Scagliusi, S. R., Sales, R. M., Caviquioli, F., and Lugão, A. B. (2019). "Study of bio-based foams prepared from PBAT/PLA reinforced with bio-calcium carbonate and compatibilized with gamma radiation," in: *Use of Gamma Radiation Techniques in Peaceful Applications*, B. A. Almayah (ed.), InTechOpen, London, UK, pp. 139-156. DOI: 10.5772/intechopen.85462

Chen, L., Ma, R., Zhang, Z., McClements, D. J., Qiu, L., Jin, Z., and Tian, Y. (2019). "Impact of frying conditions on hierarchical structures and oil absorption of normal maize starch," *Food Hydrocolloids* 97, article ID 105231. DOI: 10.1016/j.foodhyd.2019.105231

Chen, L., Tian, Y., Sun, B., Cai, C., Ma, R. and Jin, Z., (2018). "Measurement and characterization of external oil in the fried waxy maize starch granules using ATR-FTIR and XRD," *Food chemistry* 242, 131-138. DOI: 10.1016/j.foodchem.2017.09.016

Coppola, G., Gaudio, M. T., Lopresto, C. G., Calabro, V., Curcio, S., and Chakraborty, S. (2021). "Bioplastic from renewable biomass: A facile solution for a greener environment," *Earth Systems and Environment* 5, 231-251. DOI: 10.1007/s41748-021-00208-7

Cuevas-Carballo, Z., Duarte-Aranda, S., and Canché-Escamilla, G. (2019). "Properties and biodegradation of thermoplastic starch obtained from grafted starches with poly (lactic acid)," *Journal of Polymers and the Environment* 27, 2607-2617. DOI: 10.1007/s10924-019-01540-w

da Silva, J. B. A., Santana, J. S., de Almeida Lucas, A., Passador, F. R., de Sousa Costa, L. A., Pereira, F. V., and Druzian, J. I. (2019). "PBAT/TPS-nanowhiskers blends preparation and application as food packaging," *Journal of Applied Polymer Science* 136(26), article 47699. DOI: 10.1002/app.47699

Dilkes-Hoffman, L., Pratt, S., Lant, P., and Laycock, B. (2019). "The role of biodegradable plastic in solving plastic solid waste accumulation," in: *Plastics to Energy*, Elsevier, Amsterdam, Netherlands, pp. 469-505. DOI: 10.1016/B978-0-12-813140-4.00019-4

Dome, K., Podgorbunskikh, E., Bychkov, A., and Lomovsky, O. (2020). "Changes in the crystallinity degree of starch having different types of crystal structure after mechanical pretreatment," *Polymers* 12(3), article 641. DOI: 10.3390%2Fpolym12030641

Fonseca, J. M., Teleken, J. G., de Cinque Almeida, V., and da Silva, C. (2019). "Biodiesel from waste frying oils: Methods of production and purification," *Energy Conversion and Management* 184, 205-218. DOI: 10.1016/j.enconman.2019.01.061

Garalde, R. A., Thipmanee, R., Jariyasakoolroj, P., and Sane, A. (2019). "The effects of blend ratio and storage time on thermoplastic starch/poly (butylene adipate-co-terephthalate) films," *Heliyon* 5(3), article e01251. DOI: 10.1016/j.heliyon.2019.e01251

Göksungur, Y., Uzunoğulları, P., and Dağbağlı, S. (2011). "Optimization of pullulan production from hydrolysed potato starch waste by response surface methodology," *Carbohydrate Polymers* 83(3), 1330-1337. DOI: 10.1016/j.carbpol.2010.09.047

Hazer, S., and Aytac, A. (2023). "Monitoring food quality-effect of curcumin in the development of polyethylene/thermoplastic starch based smart packaging," *Journal of Vinyl and Additive Technology* 29(5), 826-839. DOI: 10.1002/vnl.22004

Iriani, E. S., Sunarti, T. C., Richana, N., Mangunwidjaja, D., and Hadiyoso, A. (2012). "Utilization of corn hominy as a new source material for thermoplastic starch production," *Procedia Chemistry* 4, 245-253. DOI: 10.1016/j.proche.2012.06.034

Jesse, T., Ezeji, T., Qureshi, N., and Blaschek, H. (2002). "Production of butanol from starch-based waste packing peanuts and agricultural waste," *Journal of Industrial Microbiology and Biotechnology* 29(3), 117-123. DOI: 10.1038/sj.jim.7000285

Jiang, Z., Ho, S.-H., Wang, X., Li, Y., and Wang, C. (2021). "Application of biodegradable cellulose-based biomass materials in wastewater treatment," *Environmental Pollution* 290, article ID 118087. DOI: 10.1016/j.envpol.2021.118087

Johansson, R., Meyer, S., Whistance, J., Thompson, W., and Debnath, D. (2020). "Greenhouse gas emission reduction and cost from the United States biofuels mandate," *Renewable and Sustainable Energy Reviews* 119, article ID 109513. DOI: 10.1016/j.rser.2019.109513

Katanyoota, P., Jariyasakoolroj, P., and Sane, A. (2023). "Mechanical and barrier properties of simultaneous biaxially stretched polylactic acid/thermoplastic

starch/poly (butylene adipate-co-terephthalate) films," *Polymer Bulletin* 80(5), 5219-5237. DOI: 10.1007/s00289-022-04312-0

Kawaguchi, H., Takada, K., Elkasaby, T., Pangestu, R., Toyoshima, M., Kahar, P., Ogino, C., Kaneko, T., and Kondo, A. (2022). "Recent advances in lignocellulosic biomass white biotechnology for bioplastics," *Bioresource Technology* 344, article ID 126165. DOI: 10.1016/j.biortech.2021.126165

Kheyrandish, M., Asadollahi, M. A., Jeihanipour, A., Doostmohammadi, M., Rismani-Yazdi, H., and Karimi, K. (2015). "Direct production of acetone–butanol–ethanol from waste starch by free and immobilized *Clostridium acetobutylicum*," *Fuel* 142, 129-133. DOI: 10.1016/j.fuel.2014.11.017

Lee, S., Cho, M., Nam, J., and Lee, Y. (2006). "Melting processing of biodegradable cellulose diacetate/starch composites," *Macromolecular Symposia* 242(1), 126-130.

Lv, Z., Yu, K., Jin, S., Ke, W., Fei, C., Cui, P. and Lu, G., (2019). "Starch granules size distribution of sweet potato and their relationship with quality of dried and fried products," *Starch-Stärke* 71(5-6), article ID 1800175. DOI: 10.1002/star.201800175

Martens, B. M., Gerrits, W. J., Bruininx, E. M., and Schols, H. A. (2018). "Amylopectin structure and crystallinity explains variation in digestion kinetics of starches across botanic sources in an *in vitro* pig model," *Journal of Animal Science and Biotechnology* 9(1), 1-13. DOI: 10.1186/s40104-018-0303-8

Mecozzi, M., Pietroletti, M., Scarpiniti, M., Acquistucci, R., and Conti, M. E. (2012). "Monitoring of marine mucilage formation in Italian seas investigated by infrared spectroscopy and independent component analysis," *Environmental Monitoring and Assessment* 184, 6025-6036. DOI: 10.1007/s10661-011-2400-4

Mendes, J., Paschoalin, R., Carmona, V., Neto, A. R. S., Marques, A., Marconcini, J., Mattoso, L., Medeiros, E., and Oliveira, J. (2016). "Biodegradable polymer blends based on corn starch and thermoplastic chitosan processed by extrusion," *Carbohydrate Polymers* 137, 452-458. DOI: 10.1016/j.carbpol.2015.10.093

Mohammadi Nafchi, A., Moradpour, M., Saeidi, M., and Alias, A. K. (2013). "Thermoplastic starches: Properties, challenges, and prospects," *Starch-Stärke* 65(1-2), 61-72. DOI: 10.1002/star.201200201

Mortalò, C., Russo, P., Miorin, E., Zin, V., Paradisi, E., and Leonelli, C. (2023). "Extruded composite films based on polylactic acid and sodium alginate," *Polymer* 282, article ID 126162. DOI: 10.1016/j.polymer.2023.126162

Okolie, J. A., Nanda, S., Dalai, A. K., and Kozinski, J. A. (2021). "Chemistry and specialty industrial applications of lignocellulosic biomass," *Waste and Biomass Valorization* 12, 2145-2169. DOI: 10.1007/s12649-020-01123-0

Onyeaka, H., Mansa, R. F., Wong, C. M. V. L., and Miri, T. (2022). "Bioconversion of starch base food waste into bioethanol," *Sustainability* 14(18), article ID 11401. DOI: 10.3390/su141811401

Pérez, S., and Bertoft, E. (2010). "The molecular structures of starch components and their contribution to the architecture of starch granules: A comprehensive review," *Starch-Stärke* 62(8), 389-420. DOI: 10.1002/star.201000013

Pokorny, J. (1998). "Substrate influence on the frying process," *Grasas y Aceites* 49(3-4), 265-270. DOI: 10.3989/gya.1998.v49.i3-4.726

Purkiss, D., Allison, A. L., Lorencatto, F., Michie, S., and Miodownik, M. (2022). "The big compost experiment: Using citizen science to assess the impact and effectiveness of biodegradable and compostable plastics in UK home composting," *Frontiers in Sustainability* 3, article 942724. DOI: 10.3389/frsus.2022.942724

Rahardiyan, D., Moko, E.M., Shun, T.J. and Keong, L.C. (2023). "Thermoplastic starch (TPS) bioplastic, the green solution for single-use petroleum plastic food packaging–A review," *Enzyme and microbial technology* 168, article 110260. DOI: 10.1016/j.enzmictec.2023.110260

Ramluckan, K., Moodley, K. G., and Bux, F. (2014). "An evaluation of the efficacy of using selected solvents for the extraction of lipids from algal biomass by the soxhlet extraction method," *Fuel* 116, 103-108. DOI: 10.1016/j.fuel.2013.07.118

Sakuragi, K., Li, P., Otaka, M., and Makino, H. (2016). "Recovery of bio-oil from industrial food waste by liquefied dimethyl ether for biodiesel production," *Energies*, 9(2), article 106. DOI: 10.3390/en9020106

Santos, J. D., Brites, P., Martins, C., Nunes, C., Coimbra, M. A., Ferreira, P., and Gonçalves, I. (2023). "Starch consolidation of calcium carbonate as a tool to develop lightweight fillers for LDPE-based plastics," *International Journal of Biological Macromolecules* 226, 1021-1030. DOI: 10.1016/j.ijbiomac.2022.11.219

Shams, M., Alam, I., and Mahbub, M. S. (2021). "Plastic pollution during COVID-19: Plastic waste directives and its long-term impact on the environment," *Environmental Advances* 5, article ID 100119. DOI: 10.1016/j.envadv.2021.100119

Su, G., Chan, C., and He, J. (2022). "Enhanced biobutanol production from starch waste via orange peel doping," *Renewable Energy* 193, 576-583. DOI: 10.1016/j.renene.2022.04.096

Yoo, S., Kelley, S. S., Tilotta, D. C., and Park, S. (2018). "Structural characterization of loblolly pine derived biochar by X-ray diffraction and electron energy loss spectroscopy," *ACS Sustainable Chemistry & Engineering* 6(2), 2621-2629. DOI: 10.1021/acssuschemeng.7b04119

Article submitted: October 30, 2023; Peer review completed: December 9, 2023; Revised version received: December 26, 2023; Accepted: January 1, 2024; Published: January 9, 2024.
DOI: 10.15376/biores.19.1.1394-1409